(Draft) HT2020-12585

3D LIGHT FIELD PROJECTION AND THE ASSOCIATE 3D PHOTOLITHOGRAPHY

Sy-Bor Wen and Hongjie Zhang

Department of Mechanical Engineering, Texas A&M University College Station, TX, USA

ABSTRACT

3D light field camera has been provided as a valid method to capture 3D surface topography with a microlens array. Through inverting the propagation direction, 3D virtual image projection can also be achieved with conventional optics and a microlens array. By compressing the 3D virtual image from the microlens array with an additional lens, microscale 3D virtual image can be achieved. We propose that microscale 3D virtual image can be valuable in microscale 3D fabrication. In this study, we provide a theoretical basis to combine femtosecond laser with the above mentioned 3D virtual image reconstruction scheme to cure photopolymers. With multiphoton effects induced by femtosecond laser, we expect 3D patterning of regions inside the photopolymer can be possible. Compared with the demonstration of 3D patterning with continuous near UV light and the proposed 3D light field projection scheme, curing of photopolymer can be limited to focal points (i.e., voxel) of the projected microscale 3D surface with two photon absorption effect when femtosecond light with high enough intensity is applied. The required femtosecond light intensity is also determined in this study. We expect this new 3D photolithography method can be valuable in fast and high precision patterning of micro to macro structures in materials that are photoactive.

1. INTRODUCTION

Following the great success of 2D microfabrication of modern integrated circuits and micro electro-mechanical systems (MEMS), there is a great desire to extend 2D microfabrication techniques to 3D domains. The resulting 3D microfabrication techniques can be valuable in constructing 3D micro photonic devices, 3D integrated circuits and 3D

MEMS systems including 3D bio-MEMS systems Compared with 2D microsystems, 3D microsystems can provide the required functionality in a much compact domain. Also, 3D microsystems can achieve better process optical, electrical, mechanical and biological information that cannot be achieved with 2D systems [2]. Current 3D microfabrication mainly based on layer-by-layer stacked process of corresponding 2D fabrications such as electron beam lithography, focused ion beam and photolithography. Though such method can produce desired 3D structures in many cases, layerby-layer approach can be time consuming. Moreover, supporting struts can be required in constructing free standing structures [3]. Therefore, 3D microfabrication based on layer-by-layer 2D sometimes called 2.5D processes are microfabrication. A full 3D microfabrication should have ability to process an arbitrary position in a 3D space without considering nearby structures.

3D microfabrication satisfying the above definitions includes single spot multiphoton lithography and holographic lithography. Single spot multiphoton lithography can reach very high spatial resolution surpassing diffraction limit (~40 nm or better). By adjusting the laser spot position in a 3D space with a Galvo mirror pair and lens position adjustment, 3D fabrication can be conducted at arbitrary positions in a 3D space. However, it is time consuming to use single spot scanning in fabricating a large 3D domain. Holographic lithography, on the other hand, can pattern 3D structures in few light projections. However, coherent light source required in holographic lithography can cause light speckles that can significantly reduce the spatial resolution in 3D microfabrication. In other words, a 3D fabrication technique that can pattern 3D microscale structures

with high speed and speckle-free structures is still missing. Based on this understanding, we are proposing a microlens array (MLA) based 3D photolithography system that have a capability of projecting 3D microscale structures without forming speckles.

MLA based 3D light field projection was inspired by the light field cameras [4,5]. Light field cameras achieve 3D imaging by inserting a MLA into traditional cameras to resolve both position and direction of recorded light rays. Through inverting the operation direction of a light field camera, 3D light field projection can also be achieved. 3D light field projection can reconstruct 3D virtual objection in a free space with MLAs. MLA based 3D light field projection has been demonstrated in a near-eye display system [6] and a volumetric light field excitation system [7]. However, there is no report showing a usage of 3D light field projection in photolithography. Though MLA based 3D light field projection has a great potential to project 3D virtual photopolymers achieve objects in to photolithography, light absorption in the photopolymer can attenuate the delivered light intensity to be delivered to the designed 3D surface. In addition, the light absorption in the photopolymer before arriving to the designed focal spots can cause unwilling curing of the photopolymer along the optical path of the incoming rays. To solve this potential issue, two photon absorption with femtosecond light source can be applied. With two photon light absorption, incoming ray has a wavelength of near IR that cannot be absorbed by the photopolymer. At the designed focal spots on a 3D surface, the associated high near IR light intensity can induce two photon absorption and then cure the photopolymer only at the focal spots.

As a short summary, we expect a combination of MLA based 3D light field projection and near IR femtosecond light can help us to achieve high speed speckle free 3D lithography and the associated 3D microfabrication. In the following sections, we will described a) the physical basis of 3D light field projection, b) theoretical analysis of a focal spot (i.e., voxel) with the proposed 3D light field projection, c) 3D patterns generated with 3D light field projection and an UV LED, and d) predictions of experimental conditions for achieving 3D light field projection with a near IR femtosecond laser.

2. PHYSICAL BASIS OF 3D LIGHT FIELD PROJECTION

In the proposed MLA based 3D light field projection system, a microlens array is placed within one focal distance away from the spatial light

modulator. The spatial light modulator can control on and off states of each pixel individually. With appropriate control of light propagating direction from the SLM, nearly parallel beam can be delivered from turned on SLM pixel to the corresponding microlens as illustrated in Figure 1.

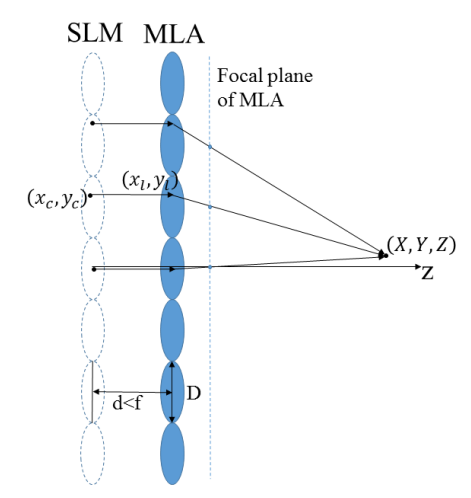


Figure 1. 3D light field projection system.

For an intended projection point (X, Y, Z) in a 3D space, the turned on SLM pixel location (x_c, y_c) beneath microlens having its center at at (x_l, y_l) should satisfy

$$x_{c} = \frac{(x_{l} - X) \times Z}{Z - f} + X$$

$$y_{c} = \frac{(y_{l} - Y) \times Z}{Z - f} + Y$$
(1)

with f the focusing distance of the microlens. Due to the limited numerical aperture of the microlens, microlenses and the associated pixels of SLM for projecting a voxel at (X, Y, Z) should satisfy

$$\sqrt{(x_l - X)^2 + (y_l - Y)^2} \le \frac{D(Z - f)}{2f}$$
 (2)

with D the diameter of each microlens.

When multiple rays strike the voxel position (X, Y, Z) simultaneously, high light intensity at the voxel position can be achieved. In following studies, we will use around 10 rays to construct one voxel in the 3D space. To construct a 3D surface in the 3D space, we first, discretize the 3D surface as a combination of voxels (i.e., point clouds in 3D space). Then, for each voxel, we can determine the active microlenses and corresponding SLM pixels to be turned on based on

Equation (1) and (2). The resulting pixel map to be turned on is then loaded in the SLM in order to reconstruct a 3D virtual object in the 3D space at designed locations.

3. THEORETICALLY DETERMINE THE VOXEL SIZE WITH DIFFRACTION INTEGRAL

To calculate the voxel size formed with the proposed 3D light field projection described above, diffraction integral with Fresnel approximation is applied. In this approach, amplitude of electric field from a given source can be expressed as [8]

$$E(x,y,z) = \frac{e^{ikz}}{i\lambda z} \iint E(x',y',z) e^{\frac{ik}{2z} \left[(x-x')^2 + (y-y')^2 \right]} dx' dy'$$
(3)

where k is the wavenumber, λ is the wavelength, E(x', y', z) is the source electric field. As a first order approximation, we assume the source electric field are square pixels as diffuse light sources behind the microlenses. The position (x_c, y_c) of each pixel behind the microlens is determined with Equation (1).

With the understanding that each microlens has very small numerical aperture, thin lens approximation can be applied in the diffraction calculation. Under this assumption, phase shift induced by each microlens can be expressed as [9]

$$phase shift = e^{-\frac{ikr^2}{2f}}$$
 (4)

with r the radial distance on the microlens with respect to its optical axis.

Combining Equations (3) and (4), the electric field generated by an appropriate SLM pixel behind the microlens centered at position (x_l,y_l) for delivering light to voxel (X,Y,Z) can be expressed as

$$E(x, y, z) = \frac{e^{ikz}}{i\lambda z} \iint e^{-\frac{ik\left[(x'-x_{i})^{2}+(y'-y_{i})^{2}\right]}{2f}} e^{\frac{ik}{2z}\left[(x-x')^{2}+(y-y')^{2}\right]} dx' dy'$$
(5)

Integration domain of the above integral is equal to one square pixel around the position (x_c, y_c) . Conductive current due to the presence of electric field can be estimated as σE with σ as the effective electrical conductivity of the target material. The associated joule heating rate inside the target is equal to $\sigma |E|^2$, that is approximately the same level

as light absorption rate inside the target (e.g., photopolymer). For a voxel formed with multiple beam intersections, the corresponding photon absorption rate can be estimated as

$$\sigma \sum_{n=1}^{m} \left| E_n(x, y, z) \right|^2 \tag{6}$$

with n as the index for the electric field generated by nth light beam. In other words, we can estimate the voxel size and the associated cured photopolymer region under appropriate light intensity through plotting the distribution of $\sum_{n=1}^{m} |E_n(x,y,z)|^2$.

Figure 2 shows
$$\sum_{n=1}^{m} |E_n(x, y, z)|^2$$
 distribution

induced by 9 intersected beams from 9 different microlenses (with locations illustrated in Figure 3) when the designed voxel position is 24 mm away from the surface of MLAs.

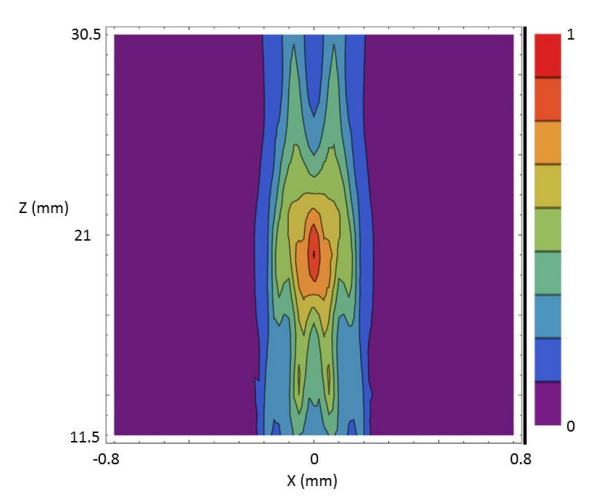


Figure 2 $\sum_{n=1}^{m} |E_n(x, y, z)|^2$ distribution at 24 mm away

from a MLA induced by 9 intersected beams. Incoming beams are from the top of the figure. FWHM is close to the contour for the green region of the plot.

Diameter and focal distance of mircrolenses used in the above calculation are $300\mu m$ and 4.8 mm respectively. Such MLA is available from Edmund Optics. The alignment of the 9 microlenses used in the light projection are illustrated in Figure 3.

Based on Figure 2, full width half maximum (FWHM) of voxel size and the associated cured photopolymer region can be estimated as 0.6 mm wide and 4 mm long. The very slender voxel shape can be attributed to the small numerical aperture of the microlenses used in the simulation. Note that

pixel illumination of SLM is assumed as diffusive light source in the diffraction integration. In real applications, light from SLM can be highly directional with an additional spatial light filter [10]. In addition to that, the focal spot size can be further reduced by compressing the projected voxels with an infinitely corrected microscope. For example, the FWHM of the voxel size can be reduced to 37.5 μm and 250 μm, respectively, when an infinitely corrected microscope with 16x image compression is applied to compress the voxel size.

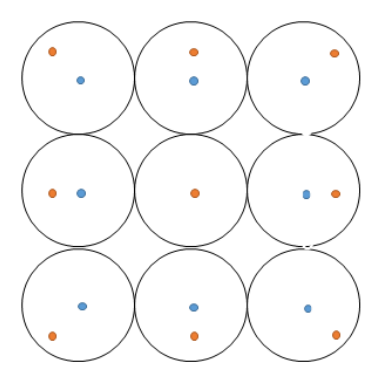


Figure 3 Arrangement of 9 microlenses used to get single voxel projection at 24 mm after the MLA surface. Blue dots are the center positions of microlenses. Red dots are the locations of turned on SLM pixels

Though it is possible to use single photon absorption with 3D light field projection to achieve 3D patterning of photopolymers, portion of photon energy from SLM can be dissipated in the photopolymer before arriving to the designed voxel position. As a result, undesired curing of photopolymers can happen at regions away from of the voxel position when the light intensity is strong enough.

One possible solution will be through two photon light absorption. By using longer wavelength (e.g., ~ 600 nm to 800 nm) femtosecond light, photon absorption before arriving to the designed voxel point can be prevented. With high enough light density, two photon light absorption can be still induced at the voxel spot. Two photon light absorption rate is

proportional to
$$\sum_{n=1}^{m} |E_n(x, y, z)|^4$$
 compared with

$$\sum_{n=1}^{m} |E_n(x, y, z)|^2$$
 for single photon light absorption as

described in previous paragraphs. Therefore, we can estimate the voxel spot from two photon light absorption using the spatial distribution of

$$\sum_{n=1}^{m} \left| E_n(x, y, z) \right|^4 \quad . \quad \text{Figure 4 shows the spatial}$$

distribution of
$$\sum_{n=1}^{m} |E_n(x, y, z)|^4$$
 generated with the

same optical alignment as for Figure 2 (i.e., 9 microlenses for generating a voxel 24 mm away from the central lens. Five pixels are turned on at each (x_c, y_c) position on SLM determined with Equation (1)). The selected wavelength is 780 nm that is commonly used in Ti:Sapphire femtosecond lasers. As illustrated in Figure 4, FWHM of the width and length of two photon voxel are reduced to 0.2 mm and 2.5 mm, respectively for two photon absorption.

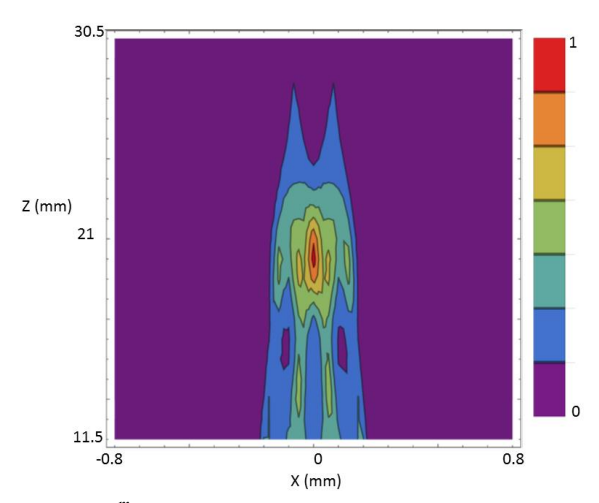


Figure 4 $\sum_{n=1}^{m} |E_n(x, y, z)|^4$ distribution at 24 mm away

from a MLA induced by 9 intersected beams. Incoming beams are from the top of the figure. FWHM is close to the contour for the green region of the plot.

Therefore, by using two photon light absorption, we not only can prevent the unwilling photon absorption before arriving the designed voxel positions, the effective voxel size can also be reduced. With a second stage optical compression with a 16x infinity corrected optical microscope, the voxel size can be further reduced to $\sim 12.5~\mu m$ and $\sim 156~\mu m$ in width and length direction, respectively.

There are two main approaches that can reduce the length of project vowels. First, MLA with larger numerical aperture can be applied. Second, the second stage infinity corrected microscope for compression purpose can be replaced with a lens providing larger magnification in the longitudinal direction than the lateral direction. For example, a single piece lens providing 16X demagnification in the lateral direction can have 256X demagnification

in the longitudinal direction based on Gaussian lens formula.

4. EXPERIMENTAL TEST

To verify the possibility of the proposed 3D light projection with microlens array photolithography, the experimental system illustrated in Figure 5 is constructed. Light is delivered to a digital mirror device working as a SLM. 3D surfaces to be projected are divided into a combination of voxels in the 3D space as in Figure 6. Pixels of SLM to be turned-on during the light field projection are determined from Equation (1). Light from selected pixels of SLM is delivered through appropriate microlenses to designed voxel locations. Figure 7 shows the pixel map to be turned on at the SLM when a 3D cone surface (Figure 6) is projected. The dimension of the 3D cone surface is 300µm tall and 250µm in base diameter. To compress the voxel size as well as the total restructured 3D structures, projected 3D virtual object is delivered to a telecentric lens pair constructed with 200 mm tube lens and 16x infinity corrected objective lens. To verify the possibility of 3D photolithography with this new 3D light projection scheme, the compressed light pattern is delivered to a 250 µm thick Su-8 photoresist layer.

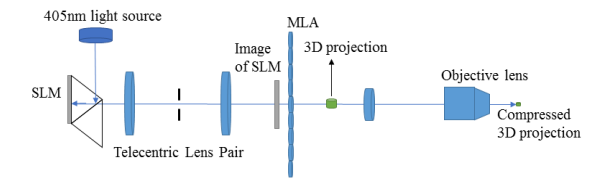


Figure 5 Experimental system of 3D light field projection

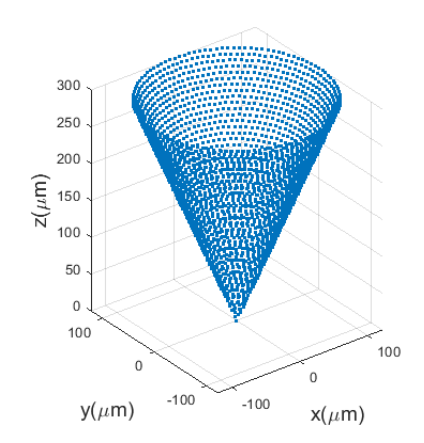


Figure 6 A point cloud to project a 3D cone surface with MLA

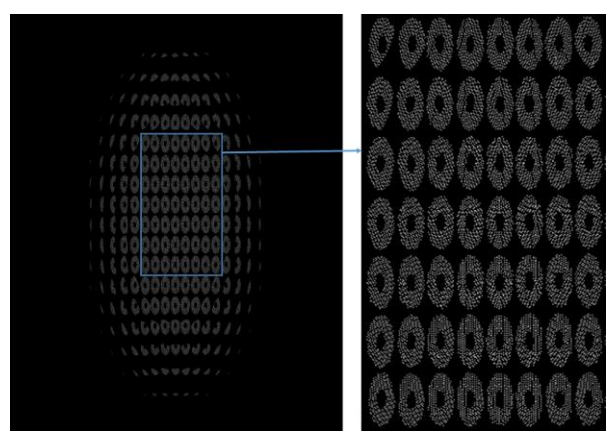


Figure 7 Pixel map of SLM when a 3D cone surface is projected

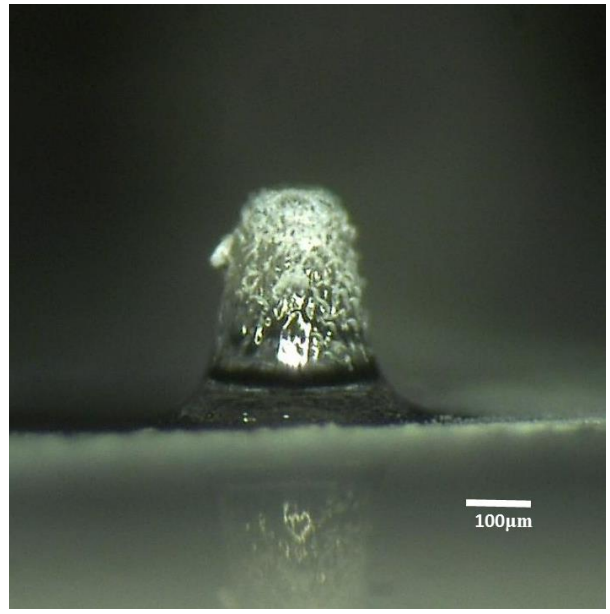


Figure 8 Cured pattern of SU-8 after development

In the test, 405 nm LED light is supplied to the SLM, that is capable to cure the SU-8 with single photon absorption. The resulting cured pattern after development is shown in Figure 8. The tapering angle of the fabricated cone is 9.8 degrees, which is different from the designed 22 degrees. Such deviation can be attributed to the unwilling curing of the SU-8 during the transport of the light beam to the designed voxel positions in the SU-8 photoresist layer.

The next step of the experiment will be replacing continuous illumination from a 405 nm LED light to femtosecond laser illumination. A coherent fs laser operating at 780 nm wavelength with ~10 fs pulse duration will be applied and is available at TAMU. Two photon absorption coefficient of SU-8 at this near IR range is ~28 (cm/TW) [11].

The imaginary part of complex permittivity of material can be expressed as a function of two photon absorption coefficient β_{TPA} as [12]

$$\varepsilon'' = \frac{c^2 \varepsilon_o n^2 \beta_{TPA}}{2\omega} |E|^2 \tag{7}$$

Since $\varepsilon'' = \frac{\sigma}{\omega}$ with σ the electric conductivity, the effectivity electric conductivity of material induced by two photon absorption is $\sigma = \frac{c^2 \varepsilon_o n^2 \beta_{TPA}}{2} |E|^2$. As a result, effective conductivity current density induced by two photon absorption can be estimated as $\frac{c^2 \varepsilon_o n^2 \beta_{TPA}}{2} |E|^2$. The corresponding energy dissipation rate in the material due to two photon absorption can be estimated as $\frac{c^2 \varepsilon_o n^2 \beta_{TPA}}{2} |E|^4$.

With the exposure dose of SU-8 as $400 \text{ mJ}/\text{cm}^2$ when the film thickness is 50 µm, we can estimate the required curing energy density for SU-8 is $\sim 8 \times 10^7 J/m^3$ based on the above equation with the refractive index n of SU-8 around 1.56. To achieve the required level of photon energy density, electric field strength generated by a fs laser with ~10 fs pulse duration should be $\sim 1 \times 10^7 V/m$. In other words, the laser fluence delivered to each voxel should be $\sim 2.6 \text{ mJ/m}^2$ (or above) in order to cure the corresponding 3D structures in SU-8 during the 3D light field projection with femtosecond laser. Assuming each voxel is constructed with ~10 beams delivered from ~10 different pixels, the required light fluence provided by each single pixel of SLM to the corresponding voxel for 3D projection is ~0.26 mJ/m². The corresponding energy from each pixel is ~0.04 nJ considering the cross-sectional area of each beam when arrives to the voxel is ~12.5 µm (after compression with the infinity-corrected microscope as described in the theoretical section). Such energy level is comparable with previous single spot two photolithography. For a common SLM with 1 million pixels, the required laser energy to be delivered to the SLM will be 40 µJ. The required 40 μJ fs laser energy can be achieved with available Ti:Sapphire fs laser system in TAMU. The required laser energy can be further reduced when

- 1. Multiple fs laser pulses are delivered to the SLM for curing same 3D region in the SU-8 layer,
- 2. Using multiple SLM pixels to generate the rays from each microlens, and

3. Using larger compression ratio objective lens to reduce the sizes of voxels projected in SU-8 layer.

5. CONCLUSION

We have proposed a new type of 3D photolithography based on 3D light field projection through a combination of SLM and MLA. With diffraction integral, it is theoretically determined the voxel size and shape that can be constructed with the proposed 3D light field projection under single and two photon absorptions, respectively. To verify this new method, an experimental system based on digital mirror device (DMD) acting as SLM, a MLA from Edmund Optics and a 405 nm LED is established in conjunction with a 16X magnification infinity corrected optical microscope. The combination of SLM, MLA and near UV LED light allows us to reconstruct 3D virtual object. The reconstructed 3D virtual object is then compressed with the infinity corrected microscope and delivered to a 250 µm thick SU-8 film. A tapered cone is successfully developed with the new 3D projection scheme. However, the shape of cone does not exactly agree with the projected optical pattern. It is expected that this size deviation can be due to the unwilling UV light absorption in the SU-8 layer before arriving to the designed voxel spots. We further propose that the unwilling absorption can be prevented through replacing the near UV LED light with near IR fs light. By using near IR fs light, absorption in the SU-8 can be prevented. With high enough fs light intensity, two photon absorption can be induced in the SU-8 only around the designed voxel positions. Through a theoretical analysis, we determined the required fs pulsed energy to achieved fs 3D light field projection and the associated fs 3D light field lithography is ~40 μJ per pulse when the pulse duration is ~10 fs. Experimental results based on the determined fs laser condition in this study will be presented in the near

To solve the very large voxel size generated with the proposed 3D light field projection/lithography especially before the compression with a second stage infinitely corrected optical microscope, we will pursue the following three approaches in the next design of 3D light field projection system.

- 1. Use MLA with larger numerical aperture. The voxel size can be reduced especially in the longitudinal direction with MLA having larger numerical aperture since the incident light beams for each voxel can be have larger incident angles to the design voxels.
- 2. Use second stage lens with large magnification ratio especially in the longitudinal

direction to further reduce the width and length of the constructed voxels in a 3D space.

3. Use SLM that that can control light emission wave front (i.e., phase controlled SLM) in additional to the amplitude control. With a properly control of the light emitting wave front from the SLM, delivered light from the SLM can be highly collimated after the microlenses. Noe that highly collimated beams can generate much smaller voxels in the 3D space. Current setup of 3D light field projection has little control on the light emission direction from the SLM and beams expand rapidly after passing through the focal point of the microlenses

ACKNOWLEDGEMENT

The authors would like to thank the National Science Foundation for the financial support with grant

REFERENCE

[1] Zhu, Wei, Christopher Obrien, Joseph R Obrien, and Lijie Grace Zhang. "3D Nano/Microfabrication Techniques and Nanobiomaterials for Neural Tissue Regeneration." Nanomedicine 9, no. 6 (2014): 859–75. https://doi.org/10.2217/nnm.14.36.

[2] Huh, Dongeun, Geraldine A. Hamilton, and Donald E. Ingber. "From 3D Cell Culture to Organson-Chips." Trends in Cell Biology 21, no. 12 (2011): 745–54. https://doi.org/10.1016/j.tcb.2011.09.005.
[3] Choi, Jae-Won, Ho-Chan Kim, and Ryan Wicker. "Multi-Material Stereolithography." Journal of Materials Processing Technology 211, no. 3 (2011): 318–28.

https://doi.org/10.1016/j.jmatprotec.2010.10.003. [4] Adelson, E. H., and J. Y. A. Wang. "Single lens stereo with a plenoptic camera." Cambridge, MA: Vision and Modeling Group, Media Laboratory, Massachusetts Institute of Technology, 1992 [5] Georgiev, T. G., and A. Lumsdaine. "Superresolution with Plenoptic 2.0 Cameras." Frontiers in Optics 2009/Laser Science XXV/Fall 2009 OSA Optics & Photonics Technical Digest, 2009. doi:10.1364/srs.2009.stua6.

[6] Lanman, Douglas, and David Luebke. "Near-eye Light Field Displays." ACM SIGGRAPH 2013 Talks on - SIGGRAPH 13, 2013. doi:10.1145/2504459.2504472.

[7] Schedl, David C., and Oliver Bimber.
"Volumetric Light-Field Excitation." Scientific Reports 6, no. 1 (2016). doi:10.1038/srep29193.
[8] Bin, Zhao, and Li Zhu. "Diffraction Property of an Axicon in Oblique Illumination." Applied Optics

37, no. 13 (January 1998): 2563. https://doi.org/10.1364/ao.37.002563. [9] Pitris, Constantinos, and Nimmi Ramanujam. Handbook of Biomedical Optics. Hoboken: Taylor and Francis, 2012. [10] Zhang, Hongjie, and Sy-Bor Wen. "Microlens Array Based Three-Dimensional Light Field Projection and Possible Applications in Photolithography." Optifab 2019, 2019. https://doi.org/10.1117/12.2536951. [11] Chowdhury, Zahidur R., and Robert Fedosejevs. "Two Photon Absorption Coefficients and Processing Parameters for Photoresists." Microsystem Technologies 14, no. 1 (April 2007): 59-67. https://doi.org/10.1007/s00542-007-0394-1. [12] Suzuki, Nobuo. "FDTD Analysis of Two-Photon Absorption and Free-Carrier Absorption in Si High-Index-Contrast Waveguides." Journal of Lightwave Technology 25, no. 9 (2007): 2495-2501. https://doi.org/10.1109/jlt.2007.903298.